Applied Nanoscience (2023) 13:6811–6818
https://doi.org/10.1007/s13204-023-02778-6

ORIGINAL ARTICLE

Application of the nanostructured R-AgLAFE electrode to study the electroreduction process of Bi(III) ions in the presence of N-acetylcysteine

Agnieszka Nosal-Wiercińska[1] · Marlena Martyna[1] · Alicja Pawlak[1] · Radosław Porada[2] · Bogusław Baś[3]

Received: 30 November 2022 / Accepted: 21 January 2023 / Published online: 13 February 2023

Abstract
Bi(III) ions electroreduction in the presence of N-acetylcysteine (ACYS)at the nanostructured R-AgLAFE electrode has been studied by the voltammetric and impedance measurements. The experimental data indicates the multistage character of the electrode process and the catalytic influence of N-acetylcysteine on the Bi(III) ions electroreduction rate. It was found that this process is controlled by the chemical reaction of the Bi(III)–$Hg(SR)_2$ activecomplexes formation on the electrode surface, which mediates electron transfer. Active complexes are a substrate in the process of electroreduction, and their different structure and properties are the reason for the diverse catalytic activity of N-acetylcysteine.

Keywords R-AgLAFE sensor · N-acetylcysteine · Active complexes · Catalytic activity · Bi(III) ions

Introduction

Due to its low toxicity and distinguished features, bismuth has been commonly used in many branches of modern industry, especially as a replacement for harmful lead. It includes the production of pigments, catalysts, fuse wire (Wexler 2014), and pseudo capacitors (Vadivel et al. 2022; Lambert 1991). Since the introduction by Wang in 2000 (Wang et al. 2000), bismuth film electrodes have been employed in the voltammetric analysis of miscellaneous inorganic (Petovar et al. 2018) and organic (Kreft et al. 2012) species. Furthermore, bismuth compounds are used in the treatment of gastro-intestinal (Woods and Fowler 1987); Shahbazi et al. 2020) and sexually transmitted diseases (Nordberg et al. 2015), as well as eyes infections (Nosal-Wiercińska 2010). The exposure and administration of bismuth compounds may result in renal dysfunction (nephrotoxicity) (Leussink et al. 2002) and influence metabolic processes, like the affect biosynthesis of heme inside the liver and kidney (Kaur and Srivastava 2014). Thus, there is a need for the development of new analytical methods, which will enable the detection and determination of Bi in biological fluids and environmental samples.

Since bismuth belongs a group of electrochemically active species, the application of electrochemical methods, especially voltammetry, for its determination is unreservedly justified. The sensitivity and detection limit of the determination can be improved by utilization of (electro) catalytic effects (Porada et al. 2020). According to the "*cap-pair*" *rule*, established in 1978 by Sykut (Sykut et al. 1978), organic substances accelerate the electrode processes, if they are able to build a stable, nanosized complex with the depolarizer, and the reduction potential of the depolarizer is located within the range of labile adsorption equilibrium (Nosal-Wiercińska 2014). The overall process consists of several homogenous chemical reactions and heterogenous electron transfer steps (Nosal-Wiercińska 2014).

The first of the above-mentioned conditions of the "*cap-pair*" ruleis in particular fulfilled for compounds containing nitrogen or sulphur atoms, whose free electron pairs form coordination bonds with depolarizer

✉ Agnieszka Nosal-Wiercińska
agnieszka.nosal-wiercinska@mail.umcs.pl

[1] Department of Analytical Chemistry, Institute of Chemical Sciences, Faculty of Chemistry, Maria Curie-Sklodowska University, Maria Curie-Sklodowska Sq. 3, 20-031 Lublin, Poland

[2] Department of Analytical Chemistry, Faculty of Chemistry, Jagiellonian University, Gronostajowa 2, 30-387 Kraków, Poland

[3] Department of Analytical Chemistry, Faculty of Materials Science and Ceramics, AGH University of Science and Technology, Mickiewicza 30, 30-059 Krakow, Poland

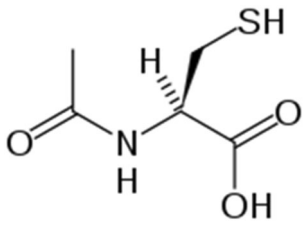

Fig. 1 N-acetylcysteine

(Nosal-Wiercińska et al. 2022a; Saba et al. 2003). This requirement is satisfied by N-acetylcysteine (ACYS) (Fig. 1), an antioxidant, which protects the cells from apoptosis, reduces the activity of some proteins, and prevents pulmonary diseases (Millea 2009; Zafarullah et al. 2003). Moreover, ACYS was found efficient in the treatment of neuropsychiatric disorders (Berk et al. 2013) and is used as neuroprotective agent in chemotherapy of colon cancer (Lin et al. 2006). Because of that, the study of electrochemical behavior of ACYS can provide a deeper understanding of its metabolic paths inside the living cell (Kaliszczak and Nosal-Wiercińska 2018).

For that purpose, the selection of an appropriate measuring system, especially the working electrode, is of utmost importance. Solid electrodes have a propensity to low reproducibility, which results from their mechanical preparation by polishing, and parameters changes in the course of an experiments due the adsorption of reagents or surface-active species (Nosal-Wiercińska et al. 2022a, b). In combination with surface roughness, these features confine the use of solid working electrodes for precise kinetics studies. In contrast to that, mercury electrodes are characterized by surface smoothness and homogeneity, and possibility to refresh the electrode surface directly before each measurement or even single measuring point, which leads to a better repeatability and reproducibility (Nosal-Wiercińska 2014; Porada et al. 2020). Nevertheless, high toxicity of mercury and legislation aimed at restriction of its usage commenced a search for its replacement with similar or improved electrochemical properties. Within this trend, several types of amalgam-based electrode constructions have been proposed (Bandžuchová et al. 2012, 2013; Baś 2006). Among them is the renewable liquid silver amalgam film electrode (R-AgLAFE), whose refreshment is realized by pulling the silver substrate electrode into the regeneration chamber, where it gets in contact with 1% (wt) liquid amalgam, followed by pushing it down to the analyzed solution. These movements are performed automatically by a pneumatic actuators and can be controlled by the AUTOLAB GPES and FRA software (Nosal-Wiercińska et al. 2021).

In this work, the detailed investigation of bismuth electroreduction on the R-AgLAFE in the presence of *N*-acetylcysteine (ACYS) in the aspect of "*cap-pair*" effect has been performed.

To that end, direct current (DC) polarography, as well as square wave (SWV) and cyclic voltammetry (CV) were employed for the determination of heterogenous rate constants, transfer coefficients, and diffusion coefficient of Bi(III)-ACYS complexes. The obtained values were compared with those inferred from the impedance spectra. This study expands the current knowledge about the kinetics of metal ions electroreduction and associated chemical processes occurring in the bulk solution.

Experimental

Materials and methods

All reagents used to make the experimental solutions: $NaClO_4$, $HClO_4$ (Sigma) and N-acetylcysteine (Sigma) were of analytical grade. The supporting electrolyte of 1 mol dm^{-3} chlorates(VII) contained 0.5 mol dm^{-3}Na $ClO_4 + 0.5$ mol dm^{-3} $HClO_4$. The choice was imposed by poor complex making properties of ClO_4^- ions, their susceptibility to water structure destruction and the fact that they adsorb only to a small extent on the mercury surface (Nosal-Wiercińska 2014). As a depolarizer, Bi(III) ions were chosen and their concentration was set to $1{\cdot}10^{-3}$ mol dm^{-3}. All of the N-acetylcysteine solutions were prepared immediately before the measurements, and their concentrations were in the range from $1{\cdot}10^{-5}$ to $1{\cdot}10^{-3}$ mol dm^{-3}. Each solution was prepared in the ultrapure water purified by the Millipore Milli-Q system and thermostated during the experiments at 298 K. Just before each measurement the samples were deaerated by high purity nitrogenin the measurement cell. Furthermore, nitrogen was passed above the solutions during the measurements.

The apparatus used to perform the electrochemical experiments was the Autolab FRA 2/GPES (Version 4.9) potentiostatwiththefrequency response analyser (Eco Chemie, Utrecht, Netherlands).

The three-electrode voltammetric cell was mounted in a programmable M165D electrode stand (mtm-anko, Cracow, Poland) and contained: the three–electrode system composed of the Ag/AgCl/3 M KCl electrode as the reference electrode, a platinum wire as the auxiliary electrode, and the cyclically renewable liquid silver amalgam film electrode (R-AgLAFE), which was renewed prior to each measurement, with the surface area of 17.25 mm^2, as the working electrode (Fig. 2).

More detailed description of the R-AgLAFE electrode refreshment before each measurement, the operating

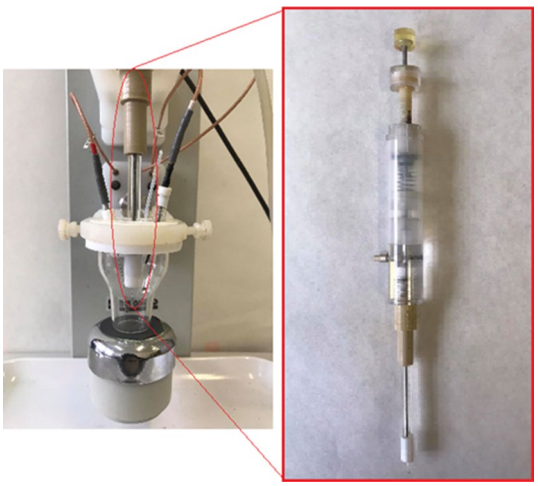

Fig. 2 Three-electrode measuring cell picture with a centrally mounted R-AgLAFE sensor (the picture on the left)

principles, and the design are presented in the paper (Nosal-Wiercińska et al. 2021).

Measurements procedure

To determine all kinetic parameters there were applied the following electrochemical techniques:

- Direct current voltammetry,
- Square wave voltammetry,
- Cyclic voltammetry,
- Electrochemical impedance spectroscopy EIS.

In the voltammetric or polarographic measurements, the optimal experimental operating conditions were as follows: the scan rate 2 mV s^{-1} for DC, the scan rate 5–1000 mV s^{-1} for the cyclic voltammetry and the step potential 2 mV, the pulse amplitude 20 mV, and the frequency 120 Hz for the square wave voltammetry. No fewer than three scans were performed for each measurement. The range of the tested potentials was constantly changed to study the variety of processes that can occur. The impedance experiments were performed in the frequency range from 50 to 50,000 Hz with the sinusoidal signal of 10 mV amplitude at the open circuit potential (OCP).

The research on the mechanism of the electrode process was associated with a need to determine the kinetic parameters: the formal potential (E_f^0)the reversible half-wave potential ($E_{1/2}{}^r$) the transfer coefficient (α)the rate constants of the depolarizer electroreduction process (k_s) and the diffusion coefficients (D_{ox})The details of the determination of the above parameters are presented in the paper (Nosal-Wiercińska 2010).

Results and discussion

Polarographic, voltammetric and impedance measurements

The SWV voltammograms recorded in the absence and in the presence of N-acetylcysteine exhibit the 5-, 9.7-, and 10.5-fold increase in the cathodic peak current for the addition of $1{\cdot}10^{-5}$, $1{\cdot}10^{-4}$, and $1{\cdot}10^{-3}$ mol dm^{-3}ACYS, respectively (Fig. 3A), which evidences the increase of Bi(III) ions electroreduction reversibility process in the chlorates(VII)

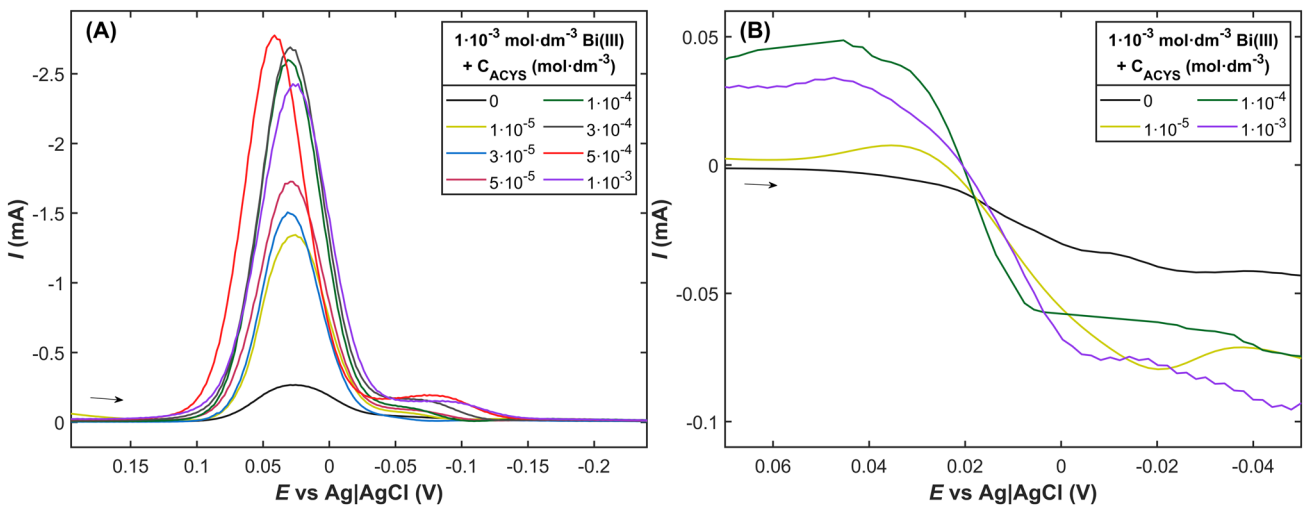

Fig. 3 **A** Square Wave voltammograms and **B** Direct Current Polarograms of the electroreduction of $1{\cdot}10^{-3}$ mol dm^{-3} Bi(III) in 1 mol dm^{-3} chlorates(VII) for various concentrations of N-acetylcysteine. The arrow indicates the direction of the scan

solution. Such an amplification in the signal is particularly valuable from the point of view of electroanalytical chemistry because it enables obtaining a lower detection limit and using greater sample dilution, thus minimalizing the matrix effect (Nosal-Wiercińska 2011; Sykut et al. 1978). The observed current increase can be ascribed to the improvement in the charge transfer rate across the electrode–electrolyte boundary which is corroborated by a higher slope of the polarographic wave at the half-wave potential (Fig. 3B) (Dalmata 2005).

The increase in reversibility of Bi(III) electroreduction in the presence of acetylcysteine in the chlorates(VII) solutions is also shown on the CV curves. In the cyclic voltammograms (Fig. 4A) there are visible two peaks, corresponding to the reduction and subsequent oxidation of Bi(III) ions, which proves that the studied process is chemically reversible.

The separation between the cathodic and anodic peaks (ΔE) recorded in the solution without ACYS is equal to 107.4 mV, indicating a hindrance in the electron transfer across the electrode–electrolyte interface. This observation is confirmed by the obtained impedance spectrum (Fig. 4B) in which only a charge transfer semicircle is pronounced (Lasia 1999).The introduction of ACYS into the measuring cell at the concentrations of $1{\cdot}10^{-5}$, $1{\cdot}10^{-4}$, and $1{\cdot}10^{-3}$ mol dm^{-3}decreasesthe value of ΔE to 34.2, 29.3, and 28.2 mV, respectively, and leads to an increase in the cathodic and anodic peaks current as well as reduces the overpotentials of the electroreduction and electrooxidation reactions, which corroborates the catalytic action of ACYS in the examined process. The impedance spectra recorded in the presence of ACYS include a semicircle, representing the charge transfer resistance (R_{ct}) as well as the adsorptive and capacitive processes at the phase boundary, and a straight line, which models the impedance of depolarizer diffusion toward the electrode surface. Such a simple comparison of the cyclic voltammograms and impedance spectra indicates that the Bi(III) electroreduction in the absence and presence of ACYS follows two different mechanisms.

To elucidate the above-mentioned differences in both mechanisms, cyclic voltammograms were recorded for the solution containing $1{\cdot}10^{-3}$ mol dm^{-3}Bi(III) using several different scan rates (Fig. 5A) and the obtained curves were subsequently analyzed in relation to the dependence of the natural logarithm of the cathodic ($\ln|I_{pc}|$, Fig. 5B) and anodic peaks current as well as the potential of the cathodic peaks (E_{pc}, Fig. 5C) on the natural logarithm of the scan rate v. As illustrated in Fig. 5A, the increase in v causes the enhancement of the cathodic and anodic peaks current, and the relationship between $\ln(|I_{pc}|)$ and ln(v) is linear with the slope of 0.418 ± 0.002 (Table 1). This value is close to the theoretical one (0.5) for the diffusion- or kinetic-controlled processes. The shift in the E_{pc} toward more negative potentials and the increase in the peak separation (ΔE, Table 2) with the rise in v prove that the rate-determining step in the investigated electroreduction of Bi(III) ions is the charge transfer across the electrode–electrolyte interface. A similar procedure was applied in the case of the cyclic voltammograms recorded in the presence of ACYS (Fig. 5D). The slopes of the $\ln(|I_{pc}|)$ vs. ln(v) dependencies (Table 1), constancy of the cathodic peaks potential and smaller changes in ΔE(Table 2) for all tested concentrations of ACYS point out to the control of

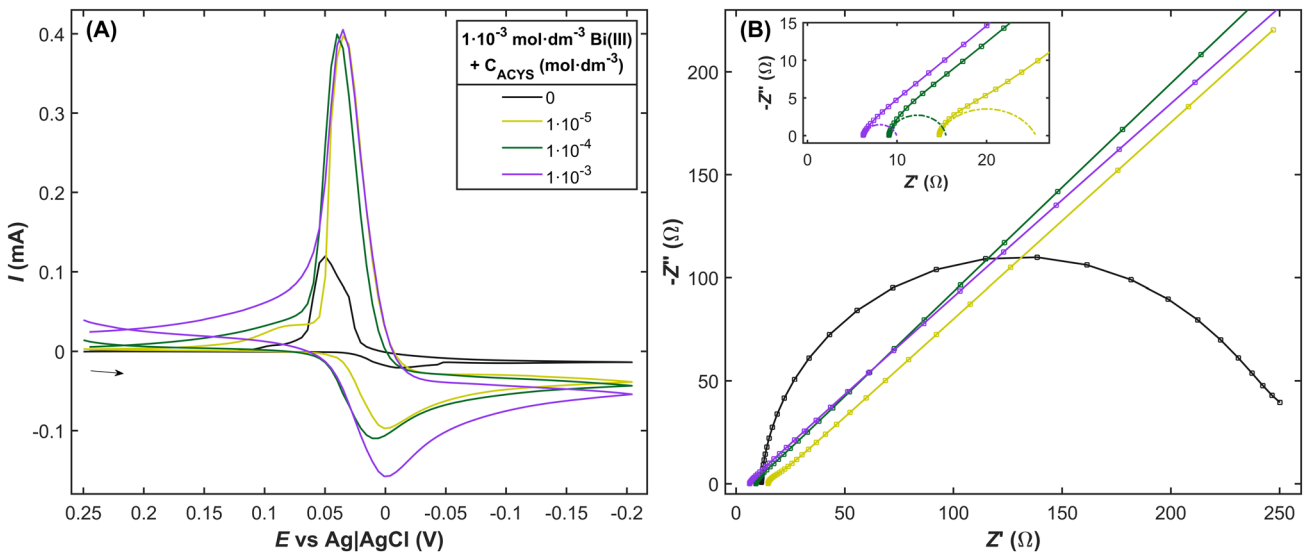

Fig. 4 **A** Cyclic voltammograms and **B** impedance spectra (registered at the E_f^0) of the electroreduction of $1{\cdot}10^{-3}$ mol·dm^{-3} Bi(III) in 1 mol dm^{-3} chlorates(VII) for various concentrations of N-acetylcysteine. The arrow indicates the direction of the scan. Scan rate $v = 50$ mV s^{-1}. Inset in **B** magnification of the spectra for low impedance value. The dashed lines represent the charge transfer semicircles

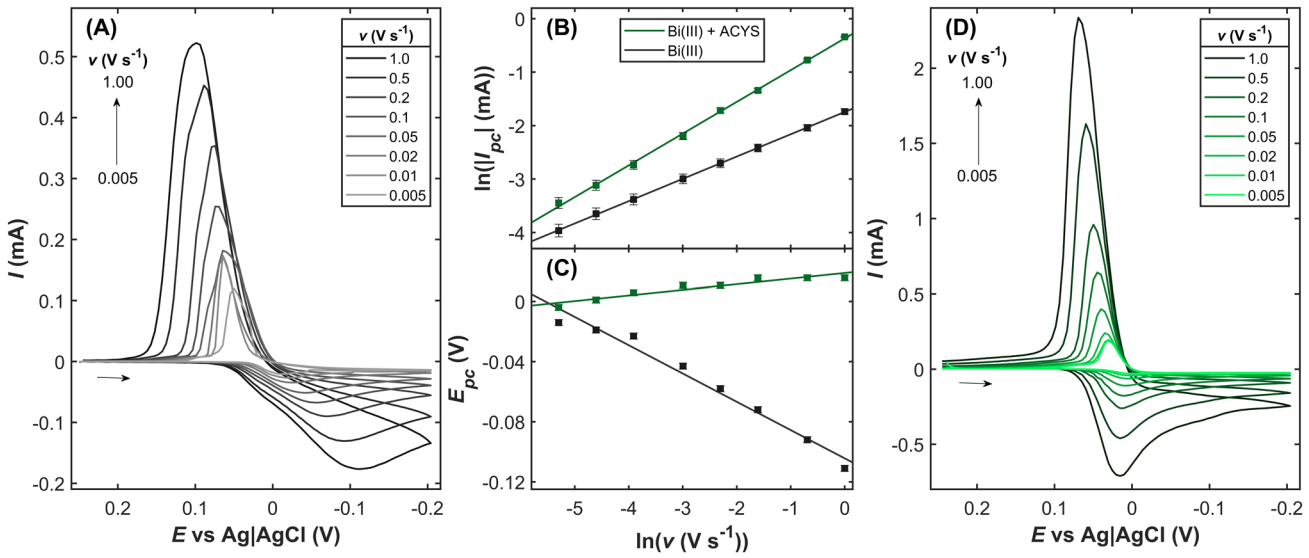

Fig. 5 Cyclic voltammograms of the electroreduction of $1{\cdot}10^{-3}$ mol dm^{-3} Bi(III) **A** in the absence and **D** in the presence of $1{\cdot}10^{-4}$ mol·dm^{-3}N-acetylcysteine. **B** The relationship between the natural logarithm of the reduction peak current (I_{pc}) and the natural logarithm of the scan rate (v). **C** The dependency of reduction peak potential (E_{pc}) on the natural logarithm of v

Table 1 The values of the slope of the dependencies of ln($|I_p|$) vs. ln(v), where I_p—peak current, v—scan rate

C_{ACYS}/mol dm^{-3}	slope	
	cathodic	*anodic*
0	0.418 ± 0.002	0.273 ± 0.025
$1{\cdot}10^{-5}$	0.528 ± 0.006	0.338 ± 0.030
$3{\cdot}10^{-5}$	0.494 ± 0.004	0.332 ± 0.032
$5{\cdot}10^{-5}$	0.649 ± 0.014	0.530 ± 0.020
$1{\cdot}10^{-4}$	0.594 ± 0.008	0.498 ± 0.033
$3{\cdot}10^{-4}$	0.605 ± 0.013	0.558 ± 0.027
$5{\cdot}10^{-4}$	0.538 ± 0.006	0.511 ± 0.022
$1{\cdot}10^{-3}$	0.525 ± 0.019	0.491 ± 0.025

the process by diffusion and influence of adsorptive processes (Porada et al. 2021).

Slight changes in the difference of anodic and cathodic peaks potentials ΔE with the changes of polarization rate (Table 2) suggest the control of the Bi(III) ions electroreduction process. The reaction is probably formation of the active Bi- catalyzing substance complexes on the electrode surface which mediate in the electron transfer (the "*cap-pair*" effect) (Nosal-Wiercińska 2011). The N-acetylcysteine adsorption on the electrode surface is favorable for formation of this complex (Fig. 6).

The course of differential capacity curves (Fig. 6) on the R-AgLAFE electrode in the 1 mol dm^{-3} chlorates(VII) solutions containing N-acetylcysteine points out to the change of differential capacity of the double layer at the R-AgLAFE/chlorates(VII) interface connected with the presence of N-acetylcysteine in the solution(Nosal-Wiercińska 2013).

Table 2 The changes in the difference between the anodic and cathodic peaks potential (ΔE) for the electroreduction of $1{\cdot}10^{-3}$ mol dm^{-3} Bi(III) in 1 mol dm^{-3} chlorates(VII) as a function of the scan rate (v) and the concentration of ACYS (C_{ACYS})

C_{ACYS}/mol dm^{-3}	ΔE/V							
	v/mV s^{-1}							
	5	10	20	50	100	200	500	1000
0	0.0791	0.0816	0.0865	0.1074	0.1270	0.1465	0.1807	0.2100
$1{\cdot}10^{-5}$	0.0391	0.0420	0.0392	0.0342	0.0420	0.0488	0.0635	0.0732
$3{\cdot}10^{-5}$	0.0391	0.0390	0.0382	0.0342	0.0391	0.0440	0.0488	0.0586
$5{\cdot}10^{-5}$	0.0293	0.0293	0.0293	0.0342	0.0342	0.0391	0.0439	0.0537
$1{\cdot}10^{-4}$	0.0342	0.0293	0.0293	0.0293	0.0342	0.0342	0.0439	0.0537
$3{\cdot}10^{-4}$	0.0293	0.0293	0.0289	0.0342	0.0391	0.0391	0.0439	0.0537
$5{\cdot}10^{-4}$	0.0293	0.0293	0.0293	0.0342	0.0342	0.0391	0.0439	0.0537
$1{\cdot}10^{-3}$	0.0338	0.0342	0.0342	0.0342	0.0391	0.0439	0.0537	0.0537

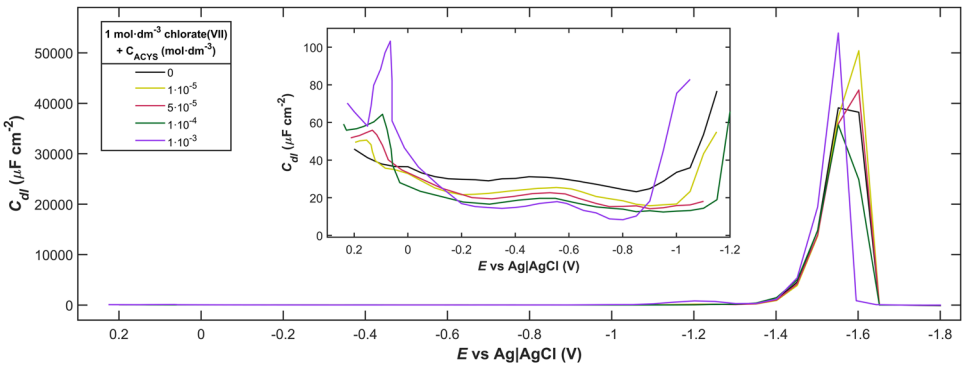

Fig. 6 Differential capacity—potential curves of double layer interface working electrode/1 mol dm^{-3}chlorates(VII) in the presence N-acetylcysteine. The concentrations of N-acetylcysteineare indicated in the figure

Referring to the N-acetylcysteine adsorption (the reactive thiol group (Fig. 1)) one can refer to the adsorption of mercury (I) and (II) cysteine thiolates (Nosal-Wiercińska 2013; Heyrovský et al. 1997) which can form an active complex with Bi(III). Thus ACYS will be a bridge in formation of such complex. Bi(III) reacts with mercury(II) cysteine thiolate $Hg(SR)_2$. This form of anodic oxidation of mercury in the presence of N-acetylcysteine is most likely to adsorb in the range of Bi(III) (~0 V) potentials reduction and is connected with the surface electrode in the labile way (Heyrovský et al. 1997). The Bi(III) ions electroreduction in 1 mol dm^{-3} chlorates(VII) in the presence of ACYS proceeds in the adsorption layer in which the active complexes of the Bi(III)–$Hg(SR)_2$ are located (Heyrovský et al. 1997). The increase in N-acetylcysteine concentration does not cause visible changes in the E_f^0 ($C_0 = 0 - E_f^0 = 0.073$ V; $C_1 = 1 \cdot 10^{-5}$ mol·$dm^{-3} - E_f^0 = 0.017$ V; $C_2 = 3 \cdot 10^{-5}$ mol $dm^{-3} - E_f^0 = 0.019$ V; $C_3 = 5 \cdot 10^{-5}$ mol $dm^{-3} - E_f^0 = 0.020$ V; $C_4 = 1 \cdot 10^{-4}$ mol $dm^{-3} - E_f^0 = 0.019$ V; $C_5 = 3 \cdot 10^{-4}$ mol $dm^{-3} - E_f^0 = 0.020$ V;). Thus, it can be concluded that there are not any stable complexes between a Bi(III) ion and N-acetylcysteine in the analyzed chlorate(VII) solutions (Ikeda et al. 1984).

The real rate constants (taking into account the influence of the double layer) of Bi(III) ion electroreduction as a function of electrode potential, determined from the impedance measurements (Fig. 7) (Souto et al. 1986), indicate that also in the presence of catalytic substances the process of Bi(III) ion electroreduction proceeds in stages. In addition, the effect of catalyst substances on the transition of the first electron is usually much greater than on the transition of the other electrons. This provides the evidence that the complexes of Bi(III) ions with the accelerating substance are already formed before the passage of the first electron which is the slowest stage and determines the speed of the entire process.

Active complexes also participate in the passage of subsequent electrons.

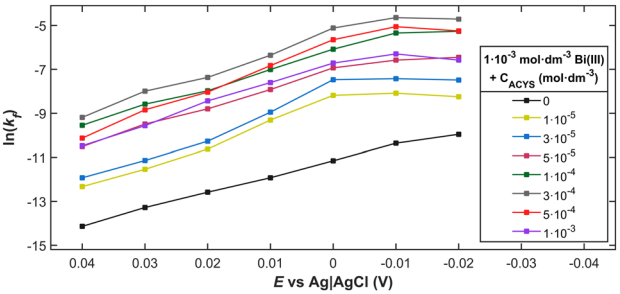

Fig. 7 Dependence of the rate constants k_f of $1 \cdot 10^{-3}$ mol dm^{-3} Bi(III) electroreduction in 1 mol dm^{-3} chlorates(VII) in the presence of N-acetylcysteine on the electrode potential. The concentrations of N-acetylcysteine are indicated on the figure

Table 3 The influence of ACYS concentration on the cathodic transition coefficients (α) and the standard rate constant (k_s) of the electroreduction of $1 \cdot 10^{-3}$ mol dm^{-3} Bi(III) in 1 mol dm^{-3} chlorates(VII)

C_{ACYS}/mol dm^{-3}	α	$10^4 k_s$/cm s^{-1}	
		CV	EIS
0	0.32	0.35	0.40
$1 \cdot 10^{-5}$	0.60	3.52	2.79
$3 \cdot 10^{-5}$	0.70	4.59	5.69
$5 \cdot 10^{-5}$	0.85	7.63	9.74
$1 \cdot 10^{-4}$	0.87	7.95	10.9
$3 \cdot 10^{-4}$	0.80	8.10	11.9
$5 \cdot 10^{-4}$	0.84	8.75	12.4
$1 \cdot 10^{-3}$	0.60	8.99	13.2

On the basis of cyclic voltammetry curves and EIS methods, the values of kinetic parameters were determined (Lasia 1999) to indicate the catalytic effect of N-acetylcysteine and its magnitude (Table 3).

An increase in the value of cathodic transition coefficients α after the introduction and with the increase of N-acetylcysteine concentration in the basic electrolyte solution indicates an increase in the reversibility of the Bi(III) ions electroreduction.

The $k_s$values confirm the catalytic effect of N-acetylcysteine on the Bi(III) ions electroreduction in the 1 mol dm^{-3} chlorates(VII) solutions. The magnitude of the catalytic effect is most likely related to the equilibrium of the reaction to form active complexes before the passage of subsequent electrons. Adsorption of the catalyst substance -as a necessary condition for accelerating the electroreduction of Bi(III) ions—does not, however, determine the magnitude of the catalytic effect. It should be noted that the values of the standard rate constants k_s determined from the CV measurements and from EIS are in good agreement.

Conclusions

Based on the study it was found that the electroreduction of Bi(III) ions in the absence and presence of ACYS is a multi-step process.

In the first case, the process is controlled by the rate of electron transfer across the R-AgLAFE electrode—chlorates(VII) solution interface.

The introduction of ACYS accelerates the electroreduction process following the "*cap-pair*" rule, according to which the charge transfer is accompanied by the preceding and following chemical reactions, including the formation of active Bi(III)—$Hg(SR)_2$ complexes.

It was shown that the Bi(III)-active complexes are already formed before the passage of the first electron which is the slowest stage and determines the rate of the whole process. Adsorption is a much faster process than kinetics or diffusion, so it is not the limiting step in the speed of the whole process. The active complexes of Bi(III) ions with the accelerating substance are formed when the hydration shell of Bi(III) ions is partially degraded. Locating close to the OHP, Bi(III) ions with a partially lost hydration envelope changes their electrostatic potential. Both the catalytic effect and its magnitude are related to the equilibrium of the reaction to form active complexes.

It was found that the mechanism of Bi (III) ion electroreduction in the presence of N-acetylcysteine involves the following stages (Nosal-Wiercińska 2014).

– Partial dehydration of Bi (III) ions and formation of active complex (I).

$$Bi\left(H_2O\right)_9^{3+} + x\left(Hg(RS)_2\right)_{ads} \rightarrow Bi\left(H_2O\right)_{(9-a)}^{3+}\left(Hg(RS)_2\right)_x + aH_2O$$

– First electron transfer.

$$Bi\left(H_2O\right)_{(9-a)}^{3+}\left(Hg(RS)_2\right)_x + e^- \rightarrow Bi\left(H_2O\right)_{(9-a)}^{2+}\left(Hg(RS)_2\right)_x$$

– Further dehydration and formation of active complex (II).

$$Bi\left(H_2O\right)_{(9-a)}^{2+}\left(Hg(RS)_2\right)_x + y\left(Hg(RS)_2\right)_{ads} \rightarrow Bi\left(H_2O\right)_{(9-a-b)}^{2+}\left(Hg(RS)_2\right)_{x+y} + bH_2O$$

– Second electron transfer.

$$Bi\left(H_2O\right)_{(9-a-b)}^{2+}\left(Hg(RS)_2\right)_{x+y} + e^- \rightarrow Bi\left(H_2O\right)_{(9-a-b)}^{+}\left(Hg(RS)_2\right)_{x+y}$$

Dehydration of Bi (I) ions and formation of active complex (III).

$$Bi\left(H_2O\right)_{(9-a-b)}^{+}\left(Hg(RS)_2\right)_{x+y} + z\left(Hg(RS)_2\right)_{ads} \rightarrow Bi^+\left(Hg(RS)_2\right)_{x+y+z} + (c)H_2O$$

Third electron transfer and amalgam formation.

$$Bi^+\left(Hg(RS)_2\right)_{x+y+z} + e^- \rightarrow Bi(Hg) + (x+y+z)\left(Hg(RS)_2\right)_{ads}$$

a + b + c = 9 and a > b > c.

Declarations

Conflict of interest The authors declare no competing interests.

References

Bandžuchová L, Šelešovská R, Navrátil T, Chýlková J, Novotný L (2012) Voltammetric monitoring of electrochemical reduction of riboflavin using silver solid amalgam electrodes. Electrochim Acta 75:316–324

Bandžuchová L, Šelešovská R, Navrátil T, Chýlková J (2013) Silver solid amalgam electrode as a tool for monitoring the electrochemical reduction of hydroxocobalamin. Electroanalysis 25:213–222

Baś B (2006) Refreshable mercury film silver based electrode for determination of chromium(VI) using catalytic adsorptive stripping voltammetry. Anal Chim Acta 570:195–201

Berk M, Malhi GS, Gray LJ, Dean OM (2013) The promise of N-acetylcysteine in neuropsychiatry. Trends Pharmacol Sci 34:167–177

Dalmata G (2005) Kinetics and mechanism of Zn (II) ions electroreduction catalyzed by organic compounds. Electroanalysis 17:789–793

Heyrovský M, MaderP VS, Veselá V, Fedurco M (1997) The anodic reactions at mercury electrodes due to cysteine. J Electroanal Chem 430:103–117

Ikeda O, Watanabe K, Taniguchi Y, Tamura H (1984) Effect of N,N′-Dimethylthiourea on the electroreduction of In(III) ions in aqueous perchlorate solutions at the mercury drop electrodes. Bull Chem Soc Jpn 57:3363

Kaliszczak W, Nosal-Wiercińska A (2018) The importance of the active complexes of 6-mercaptopurine with Bi(III) with regards to kinetics and electrode mechanism changes in the presence of non-ionic surfactants. J Electroanal Chem 828:108–115

Kaur B, Srivastava R (2014) Nano crystalline metallosilicate modified electrodes for the simultaneous, sensitive, and selective determination of riboflavin, rutin, and pyridoxine. Electroanalysis 26:1078–1089

Kreft GL, De Braga OC, Spinelli A (2012) Analytical electrochemistry of vitamin B 12 on a bismuth-film electrode surface. Electrochim Acta 83:125–132

Lambert JR (1991) Pharmacology of bismuth-containing compounds. Rev Infect Dis 13:691–695

Lasia A (1999) Electrochemical Impedance spectroscopy and its application. Modern aspects of electrochemistry. Kluwer Academic/Plenum Publishers, New York

Leussink BT, Nagelkerke JF, Nordberg GF, Van De Water B, Slikkerveer A, Van Der Voet GB, Srinivasan A, Bruijn JA, De Wolff FA, De Heer E (2002) Pathways of proximal tubular cell death in bismuth nephrotoxicity. Toxicol Appl Pharmacol 180:100–109

Lin PC, Lee MY, Wang WS, Yen CC, Chao TC, Hsiao LT, Yang MH, Chen PM, Lin KP, Chiou TJ (2006) N-acetylcysteine has neuroprotective effects against oxaliplatin-based adjuvant chemotherapy in colon cancer patients: preliminary data. Support Care Cancer 14:484–487

Millea PJ (2009) N-acetylcysteine: multiple clinical applications. Am Fam Physician 80:265–269

Nordberg GF, Fowler BA, Nordberg M (2015) Handbook on the toxicology of metals, 4th edn. Academic Press, Cambridge

Nosal-Wiercińska A (2010) The kinetics and mechanism of the electroreduction of Bi(III) ions from chlorates (VII) with varied water activity. Electrochim Acta 55:5917–5921

Nosal-Wiercińska A (2011) The catalytic activity of cysteine and cystine on the electroreduction of Bi(III) ions. J Electroanal Chem 662:298–305

Nosal-Wiercińska A (2013) The influence of water activity on double layer parameters on the interface mercury/chlorates (VII) in the presence of cysteine. Croat Chem Acta 86:159–164

Nosal-Wiercińska A (2014) Intermolecular interactions in systems containing Bi(III)-ClO-4-H_2O—selected amino acids in the aspect of catalysis of Bi(III) electroreduction. Electroanalysis 26:1013–1023

Nosal-Wiercińska A, Martyna M, Grochowski M, Baś B (2021) First electrochemical studies on "CAP—PAIR" effect for BI(III) ion electroreduction in the presence of 2-thiocytosine on novel cyclically renewable liquid silver amalgam film electrode (R-AgLAFE). J Electrochem Soc 168:066504

Nosal-Wiercińska A, Martyna M, Skrzypek S, Szabelska A, Wiśniewska M (2022a) Electroreduction of Bi(III) ions in the aspect of expanding the, cap-pair" effect: the role of the nanosized active complexes. Appl Nanosci 12:947–955

Nosal-Wiercińska A, Martyna M, Wiśniewska M (2022b) Influence of mixed 2-thiocytosine–ionic surfactants adsorption layers on kinetics and mechanism of Bi (III) ions electro reduction: use of the nanostructured R-AgLAFE. Appl Nanosci. https://doi.org/10.1007/s13204-022-02605-4

Petovar B, Xhanari K, Finšgar M (2018) A detailed electrochemical impedance spectroscopy study of a bismuth-film glassy carbon electrode for trace metal analysis. Anal Chim Acta 1004:10–21

Porada R, Jedlińska K, Lipińska J, Baś B (2020) Review—voltammetric sensors with laterally placed working electrodes: a review. J Electrochem Soc 167:037536

Porada R, Fendrych K, Baś B (2021) Electrochemical sensor based on Ni-exchanged natural zeolite/carbon black hybrid nanocomposite for determination of vitamin B6. Microchim Acta 188:323

Saba J, Nieszporek J, Gugala SD, Szaran J (2003) Influence of the mixed adsorption layer of 1-butanol/toluidine isomers on the two step electroreduction of zinc(II) ions. Electroanalysis 15:33–39

Shahbazi MA, Faghfouri L, Ferreira MPA, Figueiredo P, Maleki H, Sefat F, Hirvonen J, Santos HA (2020) The versatile biomedical applications of bismuth-based nanoparticles and composites: Therapeutic, diagnostic, biosensing, and regenerative properties. Chem Soc Rev 49:1253–1321

Souto RM, Sluyters-Rehbach M, Sluyters JH (1986) On the catalytic effect of thiourea on the electrochemical reduction of cadmium(II) ions at the DME from aqueous 1 M KF solutions. J Electroanal Chem 201:33–45

Sykut K, Dalmata G, Nowicka B, Saba J (1978) Acceleration of electrode processes by organic compounds -, cap-pair" effect. J Electroanal Chem 90:299–302

Vadivel S, Hariganesh S, Paul B, Balasubramanian N, Rajendran S (2022) Bismuth enriched materials for pseudo capacitor applications. Encycl Energy Storage 4:581–589

Wang J, Lu J, Hocevar SB, Farias PAM, Ogorevc B (2000) Bismuth-coated carbon electrodes for anodic stripping voltammetry. Anal Chem 72:3218–3222

Wexler P (2014) Encyclopedia of toxicology, 3rd edn. Academic Press, Cambridge

Woods JS, Fowler BA (1987) Alteration of mitochondrial structure and heme biosynthetic parameters in liver and kidney cells by bismuth. Toxicol Appl Pharmacol 90:274–283

Zafarullah M, Li WQ, Sylvester J, Ahmad M (2003) Molecular mechanisms of N-acetylcysteine actions. Cell Mol Life Sci 60:6–20